

Aerodynamic Shape Design of Nozzles Using a Hybrid Optimization Method

X. Q. Xing and M. Damodaran

Singapore-MIT Alliance (SMA) &
Division of Thermal and Fluids Engineering
School of Mechanical and Production Engineering
Nanyang Technological University
Nanyang Avenue, Singapore 639798

Abstract— A hybrid design optimization method combining the stochastic method based on simultaneous perturbation stochastic approximation (SPSA) and the deterministic method of Broydon-Fletcher-Goldfarb-Shanno (BFGS) is developed in order to take advantage of the high efficiency of the gradient based methods and the global search capabilities of SPSA for applications in the optimal aerodynamic shape design of a three dimensional elliptic nozzle. The performance of this hybrid method is compared with that of SPSA, simulated annealing (SA) and gradient based BFGS method. The objective functions which are minimized are estimated by numerically solving the 3D Euler and Navier-Stokes equations using a TVD approach and a LU implicit scheme. Computed results show that the hybrid optimization method proposed in this study shows a promise of high computational efficiency and global search capabilities.

Index Terms—Hybrid optimization method, Simulated annealing, Gradient-based optimization, Simultaneous perturbation stochastic approximation, aerodynamic shape design, CFD.

I. INTRODUCTION

DETERMINISTIC optimization methods are efficient in finding the minima of continuously differentiable problems for which sufficiently accurate derivatives can be estimated at reasonable cost, but these methods may not lead to a global optimum and often restrict the design space to conventional designs. Besides deterministic methods,

stochastic methods such as genetic algorithm (GA), simulated annealing algorithm and SPSA etc have recently found applications in practical engineering design optimization problems. These non-deterministic algorithms are easily implemented in robust computer codes and they have the advantage of yielding a global minimum and overcome the limitations of deterministic gradient-based search methods which have a tendency of getting trapped in local minima. However, SA, SPSA and GA methods require a large number of function evaluations and relatively long computation times especially for the case of complex design problems. One approach to reduce computational time would be to use parallel optimization methods as outlined in Wang and Damodaran [1]. Although parallel optimization strategies can speedup the computation, they still need large computational resources.

Based on previous investigations on aerodynamic shape design problems, such as 2D airfoil shape design with/without constraints, 3D blade shape design problem, 2D axisymmetric nozzle shape design problem using different optimization methods including stochastic methods (SPSA and SA) and gradient based methods and hybrid methods of SPSA and BFGS [1-3], a hybrid method combining SPSA and BFGS is developed in order to find a high efficient stochastic-based method which can use the high efficiency of the gradient-based method, and the global search capability of SPSA method at the same time. A few benchmarking objective functions are selected to validate its performance. After validated, it is used to the optimal 3D nozzle aerodynamic shape design problem to maximize the thrust of the nozzle.

The performance of this hybrid method is compared with SPSA, SA and BFGS optimization methods by applying these techniques to the optimal shape design of three-dimensional elliptic nozzles in high speed compressible flows. The design objective function which is to be optimized is estimated using a finite volume compressible flow solver solving the 3D Euler and Navier-Stokes equations using a TVD approach and a LU implicit scheme.

X. Q. Xing is a Research Fellow in HPCES, Singapore-MIT Alliance, Nanyang Technological University, 50 Nanyang Avenue, Singapore, 639798, (phone: 65-67904074; e-mail: xqxing@ntu.edu.sg).

M. Damodaran, is an Associate Professor of Nanyang Technological University and a SMA Fellow of HPCES, Singapore-MIT Alliance, 50 Nanyang Avenue, Singapore, 639798, (phone: 65-67905599; e-mail: mdamodaran@ntu.edu.sg).

II. HYBRID OPTIMIZATION METHOD

A. SPSA method

SPSA is an algorithm that is based on a “simultaneous perturbation” gradient approximation. The “simultaneous perturbation” approximation uses only two function measurements independent of the number of parameters (say, p) being optimized. The SPSA algorithm works by iterating from an initial guess of the optimal vector X_0 . First, the counter index k is initialized to a value of 0, an initial guess of the design variable vector X_k and non-negative empirical coefficients are defined. Next a p -dimensional random simultaneous perturbation vector Δ_k is constructed and two measurements of the objective function, namely $y(X_k + c_k \Delta_k)$ and $y(X_k - c_k \Delta_k)$ are obtained based on the simultaneous perturbation around the given vector X_k . The parameter $c_k = c_0 / (k^m)$ where c_0 is a small positive number, k is the loop index and m is a coefficient taken as 1/6 in this study. The term Δ_k represents the random perturbation vector generated by Monte-Carlo approaches and the components of this perturbation are independently generated from a zero-mean probability distribution and a simple distribution that has been used in this study is the Bernoulli ± 1 distribution with probability of $1/2$ for each ± 1 outcome. This is followed immediately by the calculation of the gradient approximation based on two measurements of the objective function based on the simultaneous perturbation around the current value of the design variable vector. After the simultaneous perturbation, approximation to the gradient $g(X_k)$ is generated, update the design vector X_k to a new value X_{k+1} using standard SA form, i.e. $X_{k+1} = X_k - a_k * g(X_k)$. Where the parameter $a_k = a_0 / (c_0 + k)^a$, a_0 and a can be chosen to ensure effective practical performance of the algorithm. In this study a is taken as 1. Finally the algorithm is terminated if there are insignificant changes in several successive iterations or if the maximum allowable number of iterations has been reached. The details of the step-by-step implementation of the SPSA algorithm are outlined in Spall [4-6]. The choice of the coefficients and parameters pertaining to the algorithm is critical for the performance of SPSA (as is the case with the choice of coefficients and parameters pertaining to all other stochastic optimization algorithms such as Simulated Annealing). Spall offered some practical suggestions for choosing the values of these coefficients and parameters.

B. Hybrid Optimization Method

The motivation for using hybrid methods for the optimization of complex design problems stems from the

need to reduce the number of design iterations required to reach optimal configurations and the possibility of exploiting good features of the optimization methods that form the hybrid to achieve that goal. For example the application of stochastic or global optimization methods for aerodynamic airfoil shape design optimization problems require a large number of function evaluations before the global optimum is reached within some stipulated tolerance criteria. Hence there is a need to improve the efficiency of stochastic optimization methods. There are many strategies for improving the efficiency of stochastic methods. Vicini [7], Poloni [8] and Muyl et al [9] have proposed hybrid methods by combining genetic algorithms(GA) and gradient-based methods. The present authors [3] had earlier proposed a hybrid method combining SPSA and gradient-based methods, which takes advantage of SPSA’s high rate of reduction of the objective function at the inception of the design process to drive the design variables towards the optimal zone at first, and then combining with other methods to perform the final stages of the convergence towards the optimal solutions. In this study, a hybrid method is proposed to take advantage of the high efficiency of gradient-based method, and the global search capability of SPSA method to get a global optimum with a high efficiency. The BFGS method is introduced after a few design cycles of SPSA method. The approach consists of applying a few design iterations of BFGS to approximate the objective function so that the search efficiency of the hybrid method is improved while maintaining the global search character of stochastic algorithm.

III. VALIDATION OF THE HYBRID METHOD

Three test objective functions were selected to validate the hybrid method. Rastrigin’s function (F1) which has the multi-modal property is given as:

$$F1 = 10n + \sum_{i=1}^{i=n} [x_i^2 - 10 \cos(2\pi x_i)], \quad -5.12 \leq x_i \leq 5.12,$$

$$F1_{\min} = F1(0,0,0...) = 0. \quad (1)$$

For this study, Rastrigin’s function with $n=10$ design variables has been considered. Initial values of the design variables are given as $x(i) = 5.0 - i * 0.1$. The design results obtained by BFGS, hybrid SPSA-BFGS, SPSA and SA are tabulated below:

TABLE I
RESULTS OBTAINED BY DIFFERENT OPTIMIZATION METHODS (F1)

	BFGS	Hybrid (SPSA-BFGS)	SPSA	SA
Final objective function values	195	0.0	0.0	3.979 8
Function evaluations	115	537	2112	29001

The final values of the design variables obtained by BFGS, hybrid of SPSA-BFGS, SPSA and SA methods are

$$X_{BFGS}^* = [4.972717, 4.972377, 4.972208, 4.971644, 3.977996, 3.980066, 3.978140, 3.977687, 3.977622, 3.977772]^T$$

$$X_{Hybrid}^* = [1.7695^{-5}, -2.3783^{-5}, 3.3738^{-6}, 1.2283^{-6}, 1.8893^{-5}, 1.1980^{-5}, 2.0655^{-5}, -2.9817^{-5}, 1.0690^{-5}, -1.4738^{-5}]^T$$

$$X_{SPSA}^* = [-6.2801^{-7}, -1.9257^{-6}, -1.6340^{-6}, -5.7605^{-6}, 3.3716^{-7}, -9.1732^{-7}, -4.4649^{-6}, 3.0026^{-6}, -2.1213^{-6}, 4.8002^{-6}]^T$$

$$X_{SA}^* = [-2.0563^{-5}, -5.8193^{-5}, -5.3139^{-5}, -5.8705^{-5}, 0.9949, 0.9949, -7.4511^{-5}, 0.9949, -1.4380^{-6}, 5.3413^{-5}]^T$$

respectively. From table 1, it's obviously that the gradient based BFGS method gets trapped into a local minimum.

Neumaier's function (F2) is a unimodal function with a narrow ridge and a sharp tip and takes the form shown as:

$$F2 = \sum_{i=1}^{i=n} (x_i - 1)^2 - \sum_{i=2}^{i=n} x_i x_{i-1}, -n^2 \leq x_i \leq n^2,$$

$$x_{i \min} = i(n+1-i), F2_{\min} = -n(n+4)(n-1)/6. \quad (2)$$

For this study, Neumaier's function with n=10 design variables has been considered. Initial values of the design variables are given as $x(i) = 5.0 - i * 0.1$. The design results obtained by BFGS, hybrid SPSA-BFGS, SPSA and SA are tabulated below:

TABLE II
RESULTS OBTAINED BY DIFFERENT OPTIMIZATION METHODS (F2)

	BFGS	Hybrid (SPSA-BFGS)	SPSA	SA
Final objective function values	-209.93	-209.72	-201.92	-210.00
Function evaluations	132	293	50760	31001

The final values of the design variables obtained by BFGS, hybrid of SPSA-BFGS, SPSA and SA methods are

$$X_{BFGS}^* = [10.1590, 18.1739, 24.2186, 28.0877, 29.9087, 29.7825, 27.6633, 23.6807, 17.7210, 9.8701]^T$$

$$X_{Hybrid}^* = [9.6912, 17.4085, 23.2934, 27.1166, 29.0868, 29.0398, 26.9432, 23.0602, 17.2622, 9.6421]^T$$

$$X_{SPSA}^* = [8.3005, 14.7356, 19.4411, 22.5108, 24.0313, 24.0350, 22.5119, 19.4604, 14.7898, 8.319724]^T$$

$$X_{SA}^* = [9.9993, 18.012, 24.019, 28.018, 30.004, 29.993, 27.997, 23.986, 17.991, 9.9962]^T$$

respectively.

Shelkel-N function (F3) which has many local minima and which is a difficult test case for generic optimization algorithm takes the form shown as:

$$F3 = -\sum_{j=1}^{j=5} \frac{1}{\sum_{i=1}^{i=4} (x_i - a_{ij})^2 + c_j}, 0 \leq x_i \leq 10,$$

$$a_{11} = 4, a_{12} = 1, a_{13} = 8, a_{14} = 6, a_{15} = 3$$

$$a_{21} = 4, a_{22} = 1, a_{23} = 8, a_{24} = 6, a_{25} = 7$$

$$a_{31} = 4, a_{32} = 1, a_{33} = 8, a_{34} = 6, a_{35} = 3$$

$$a_{41} = 4, a_{42} = 1, a_{43} = 8, a_{44} = 6, a_{45} = 7$$

$$c_1 = .1, c_2 = .2, c_3 = .2, c_4 = .4, c_5 = .4$$

$$F3_{\min}(4,4,4,4) = -10.1532 \quad (3)$$

For this study, Shelkel-N function with n=4 design variables has been considered. Initial values of the design variables are given as $x(i) = 5.0 - i * 0.1$. The design results obtained by BFGS, hybrid SPSA-BFGS, SPSA and SA are tabulated below:

TABLE III
RESULTS OBTAINED BY DIFFERENT OPTIMIZATION METHODS (F3)

	BFGS	Hybrid (SPSA-BFGS)	SPSA	SA
Final objective function values	-10.0531	-10.0535	-10.0528	-10.0535
Function evaluations	36	94	2037	22001

The final values of the design variables obtained by BFGS, hybrid of SPSA-BFGS, SPSA and SA methods are

$$X_{BFGS}^* = [4.000254, 4.000137, 3.999283, 3.9980734]^T,$$

$$X_{Hybrid}^* = [3.999840, 3.999968, 4.000054, 4.000088]^T$$

$$, X_{SPSA}^* = [3.998549, 3.998720, 3.998559, 3.998710]^T$$

$$\text{and } X_{SA}^* = [3.999982, 3.999983, 3.999981, 3.999984]^T \text{ respectively.}$$

From the three benchmarking test functions, it can be seen that SPSA and SA method require thousands of function evaluations to reach convergence, and gradient-based BFGS method has high computational efficiency, but sometimes it gets trapped into local optimum, such as the case with Rastrigin's function. The hybrid method proposed in this study has almost same computational efficiency with BFGS method and has the capability of finding the global optima. In next section, it will be used for a nozzle shape design problem, to test its performance for engineering design optimization problems.

IV. APPLICATION OF THE HYBRID METHOD IN 3D NOZZLE SHAPE DESIGN OPTIMIZATION

Aerodynamic shape design combining modern CFD and optimization methods has potential applications in the design of airfoils and wings, flight vehicles, aerospike, wind-tunnels, nozzles, diffusers and jet engine components. The design test case chosen for the application of the hybrid method concerns the optimal design of a 3D elliptical nozzle shape. The elliptical nozzle is chosen since it is relatively simple to model and can be viewed as having applications in integral rocket ramjet, scramjet and high speed internal flow systems. In order to initiate the design process, there is a need for the parametric representation of the surfaces of the 3D elliptical nozzle shape.

A. Parameterization of 3D Nozzle Geometry

Parameterization of the shape is used for defining design parameters for initiating the design optimization. A number of choices exist for this. In this work, cubic splines as outlined in Wang and Damodaran [10] are used to define surfaces and design parameters for the shape design. Cubic splines produce an interpolated function which preserves continuity in its second derivative and smoothness in its first derivative. For the three dimensional shape design studied in this work, bi-cubic splines which interpolate one functional value alone first and which then interpolates another functional value are used to define the design variables and the shape of the surface in the 3D space. To solve the 2D problem, for the given tabulated function $y(x_i)$, ($i = 1, \dots, M$) the function value $y(x)$ formulated by the cubic splines on the interval (x_i, x_{i+1}) can be represented by

$$y(x) = Ay_i + By_{i+1} + Cy_i'' + Dy_{i+1}'' \quad (4)$$

where the A, B, C and D are the functions of $(x - x_i)$ or $(x - x_{i+1})$, the y_i'' and y_{i+1}'' are unknown which can be determined by solving a set of equations: $y_i'' = y_{i+1}''$, at point $x = x_i$, ($i=2$ to $m-1$). These continuity requirements across the boundary between the intervals (x_{i-1}, x_i) and (x_i, x_{i+1}) are defined by the cubic splines.

For establishing the bicubic splines in 3D space for the given tabulated functions $z(x_j, y_i)$, ($i=1, \dots, M, j=1, \dots, N$), one can perform a series of 1D splines for the given (expected) value y on the interval (y_j, y_{j+1}) ,

$$z(x_i, y) = Az_j + Bz_{j+1} + Cz_j'' + Dz_{j+1}'' \quad (5)$$

where the A, B, C and D are the functions of $(y - y_j)$ or $(y - y_{j+1})$, following these interpolated M points (with same y values), and z_j'' and z_{j+1}'' are solved in the same way as above. One can further interpolate x on the interval

(x_i, x_{i+1}) to formulate the bicubic splines

$$z(x, y) = \bar{A}z_i + \bar{B}z_{i+1} + \bar{C}z_i'' + \bar{D}z_{i+1}'' \quad (6)$$

where, \bar{A} , \bar{B} , \bar{C} and \bar{D} are the functions of $(x - x_i)$ or $(x - x_{i+1})$, which can be solved as same as equation (6).

Details of this procedure are outlined in Press [11]. In this study the natural cubic spline, which has zero second derivative at the inlet and outlet boundaries of the nozzle configuration, is chosen.

B. CFD Models for Estimating Objective Functions

A three-dimensional compressible CFD solver for solving the Reynolds-averaged Euler/Navier-Stokes equations is used to compute the flow field in which converged steady state solutions are obtained by time-marching scheme from the initial conditions. The computed flow field is then used to estimate the objective function which is to be optimized. In order to enhance convergence Euler/Navier-Stokes equations are solved using the LU-SGS implicit scheme proposed by Yoon and Kwak [12]. In order to improve the resolution of the computed flow field the TVD scheme proposed by Yee and Harten [13] is implemented. Details have been reported in Wang and Damodaran [10].

C. 3D Nozzle Design Using Inviscid Flow

This test case is designed for optimizing the shape of a 3D elliptical nozzle for which the inflow flow field conditions are defined. The goal is to find an optimal shape of the nozzle wall or cross-sectional area distribution along the flow direction to maximize the thrust of nozzle. The objective function $F(x)$ which is to be optimized is expressed in normalized form as follows:

$$F(x) = \int (\mathbf{r}u^2 + p) / (\mathbf{r}_0u_0^2) dS \quad (7)$$

where the dS corresponds to the elemental area $dydz$ on the exit cross section (y - z) lane. Note that $F(x)$ has been normalized by the inflow condition $\mathbf{r}_0u_0^2$, where \mathbf{r}_0 and u_0 are the inflow density and velocity respectively which are taken as reference values for scaling flow quantities in internal flow simulations using CFD analysis, and X is the vector of design variables i.e., $X = (x_1, x_2, \dots, x_{16})$. The integration is evaluated on the cross-section of nozzle exit. The flow field is calculated by numerically solving the Euler equations by the method outlined earlier on a structured 3D grid consisting of $71 \times 15 \times 15$ grid points. The inflow Mach number at the inlet is 0.926 with subsonic inflow and supersonic outflow at the nozzle exit. The Reynolds number $Re = 1.48E + 07$ based on characteristic length of major axis of ellipse of the inlet cross section. The cross-sectional areas at inlet, throat and outlet are fixed in the optimization process and are set to be ellipses. The inlet cross-sectional shape is defined by selecting the ratio of the minor axis b to the major axis a i.e. $(b/a) = 0.5/1.0$ and for the throat and

outlet their ratio is 0.45/0.90 and 1.0/2.0 respectively. Nozzle configuration consists of 16 design variables which in this case are nodes on the surface of the nozzle, the positions of which are shown in Fig. 1(a), which shows a quadrant of the nozzle.

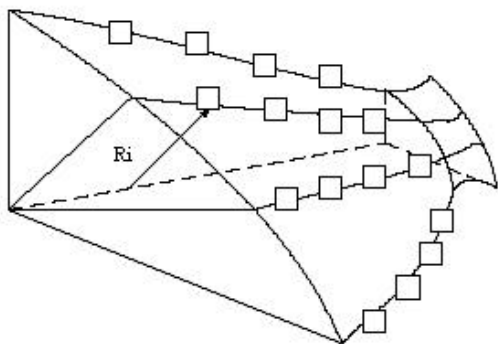


Fig 1.(a): Design variables in 3D nozzle design (one quadrant)

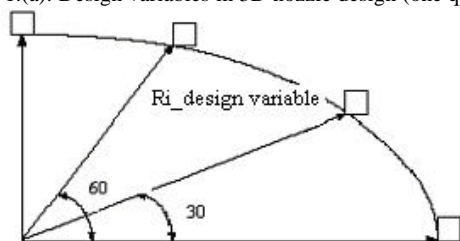


Fig. 1(b) distribution of design variables on the cross-section of the elliptical nozzle

In the design optimization process the design surface nodes are constrained not to move axially along the length of the nozzle, and are also fixed in the circumferential direction along the 0, 30, 60 and 90 degree rays emanating from the centre of the nozzle section as shown in Fig. 1(b). The 16 points are free to move along radial direction and are grouped into 4 cross-sectional planes which are uniformly located along length of nozzle as shown in Fig. 1(a). The radii R_i ($i = 1, 16$) denoted in Fig. 1(a) are the control points which are defined as the design variables to be optimized. In this study, the constraints are given in a simple way, the design variables only subject to the defined upper and lower limits. The maximization of thrust can be defined in the sense of a minimization problem $Min[1/f(x)]$.

D. 3D Nozzle Design Considering Viscous Flow

Three dimensional nozzle design considering viscous flow is also conducted for examining the efficiency of the hybrid method of SPSA and BFGS while using the Navier-Stokes equations to evaluate the objective functions and to consider the effects of viscous and turbulence on the nozzle design. The turbulent viscosity is calculated using the simple zero-equation algebraic turbulence model.

A fine grid consisting of 51x25x25 grid points is used for simulating turbulent flows. The parameters of the inflow and initial geometry of the nozzle are the same as those pertaining to the nozzle used for inviscid flow analysis.

V. RESULTS AND DISCUSSION

Optimization results obtained by solving 3D Euler/Navier-Stokes equations with BFGS, hybrid SPSA-BFGS, SPSA and SA method are given in this section.

The criteria for termination for optimization using inviscid and viscous flow solvers is to stop the program if the absolute change in the objective function between certain number of consecutive design iterations is less than 10^{-5} or if the maximum allowable number of iterations has been reached. Table IV-V show function evaluations needed by the four optimization methods and the optimal objective function values obtained by different optimization methods with inviscid and viscous flow respectively. Since, the various tuning parameters present in the optimization algorithms affect the performance of each optimization method, different values of the tuning parameters corresponding to each optimization method have been attempted to yield the best performance for this problem. All the results listed in the table and shown in the figures correspond to the tuning parameters which give the best performance for each optimization method.

Table. IV RESULTS OBTAINED BY DIFFERENT OPTIMIZATION METHODS (INVISCID FLOW)

	BFGS	Hybrid (BFGS-SPSA)	SPSA	SA
Final objective function values	3.2979	3.3042	-	3.2744
Function evaluations	130	192	-	>500

Table V RESULTS OBTAINED BY DIFFERENT OPTIMIZATION METHODS (VISCIOUS FLOW)

	BFGS	Hybrid (BFGS-SPSA)	SPSA	SA
Final objective function values	3.2594	3.2623	-	3.2607
Function evaluations	76	145	-	201

The attainment of the optimal value of the objective function using BFGS, SA, SPSA and the hybrid SPSA-BFGS method over the number of objective function evaluations is shown in Fig. 2, from which it can be seen that SPSA and SA require a greater number of function evaluations to reach the user-defined criteria for convergence termination, while BFGS and the hybrid method appear to be more efficient requiring fewer design iterations. The BFGS method requires about 130 function evaluations and the hybrid method of SPSA-BFGS proposed requires about 192 function evaluations to satisfy the objective function convergence criteria. This implies that the hybrid method of BFGS-SPSA has the almost same order of computational efficiency as the gradient-based

BFGS method for the 3D nozzle design using Euler equations based CFD model. Both BFGS and the hybrid BFGS-SPSA have high computational efficiencies compared with SA and SPSA methods. From table.1, it can be seen that the optimal function value 3.3042 obtained by the hybrid method proposed in this study is the highest when compared with the values obtained by other methods and this suggests that the design result of the hybrid method is the nearest to the global optimum.

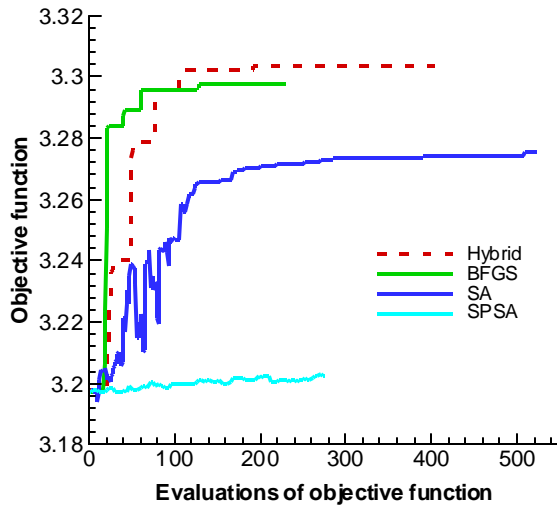


Fig.2(a) Comparison of convergence history obtained by different optimization methods with inviscid flow

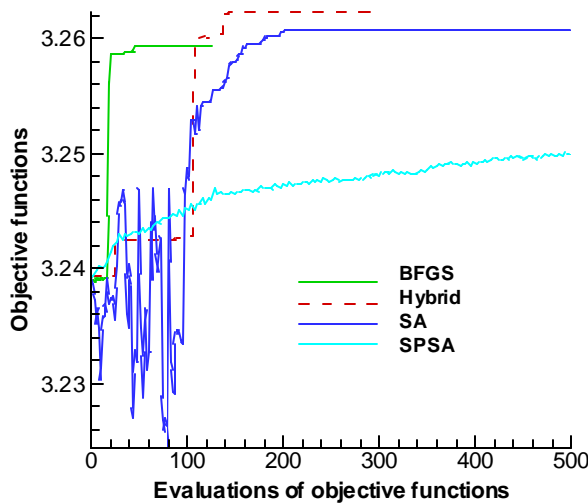


Fig.2(b) Comparison of convergence history obtained by different optimization methods with viscous flow

Fig.3 – Fig.6 show the computed optimised results obtained using the hybrid optimization method. Fig.3(a) and Fig.3(b) show the locations of the initial and final design variables in radial direction for hybrid optimisation using inviscid and viscous flow solvers for function evaluations respectively. Fig. 4(a), Fig.4(b) and Fig. 4(c) show the initial shape and the final optimized shape of the 3D elliptical nozzle using inviscid and viscous flow solvers respectively. It can be seen that the initial shape and the

optimized shape of the 3D elliptical nozzle are different since the nozzle shape has to change to give the improved thrust. It can also be seen that the final shapes obtained by optimization using inviscid and viscous flow solvers are similar. Both of them appear to have evolved a second ‘throat’ in the vicinity of the nozzle outlet. Since a finer grid in the circumferential direction is introduced, the nozzle shape obtained with viscous flow is smoother.

Fig. 5(a) and Fig. 5(b) show contours of the normalized total pressure $(ru^2 + p)/(r_0u_0^2)$ from inlet to the outlet corresponding respectively to the initial state and the final optimized state with inviscid flow. It can be seen that normalized total pressure increases near the outlet compared with the initial value. These result in improved thrust. Fig. 6(a) and Fig. 6(b) show contours of the normalized total pressure $(ru^2 + p)/(r_0u_0^2)$ from inlet to the outlet corresponding respectively to the initial state and the final optimized state with viscous flow. It can be seen that normalized total pressure increases at the exit, especially along the major axis of the section elliptical compared with the initial value and this results in improved objective function value. Optimization results of the 3D nozzle design using inviscid or viscous flow solvers verify the performance of the hybrid method, and seems to suggest that the hybrid method has the capability to find the design nearest to the global optimum for the 3D nozzle design problems, not only for the design considering inviscid flow problem, also for that considering viscous flow.

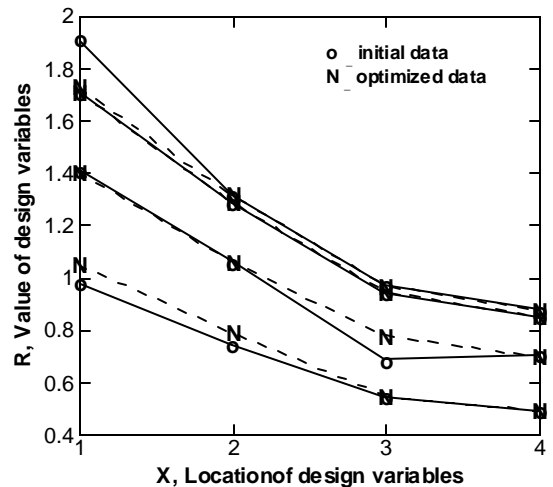


Fig.3(a). Locations of Initial and final design variables obtained by the hybrid method with inviscid flow

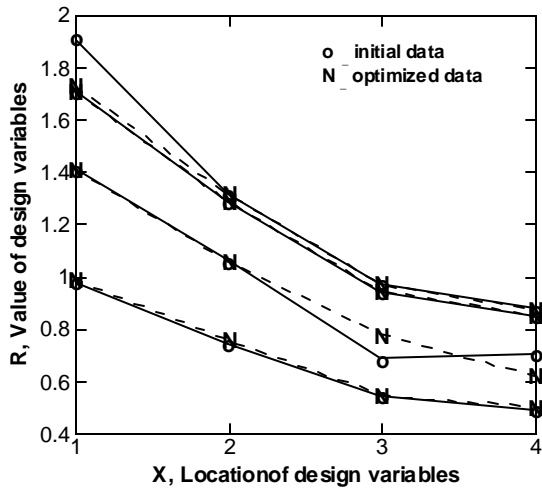


Fig.3(b). Locations of Initial and final design variables obtained by the hybrid method with viscous flow

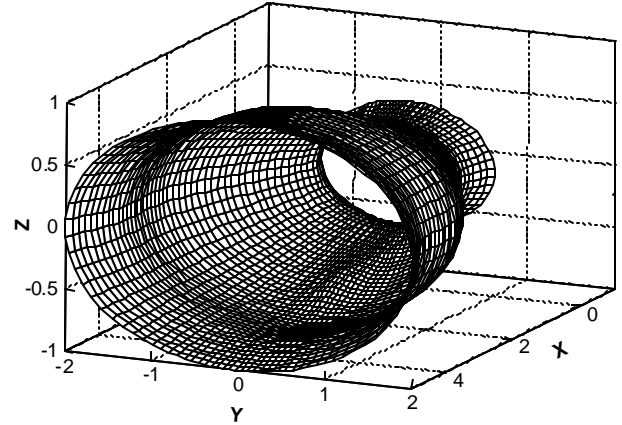


Fig.4(c) Final shape of the 3D elliptical nozzle obtained by the hybrid method with viscous flow

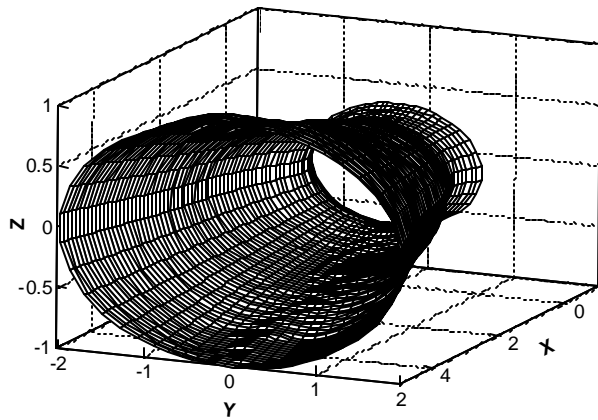


Fig.4(a) Initial shape of the 3D elliptical nozzle

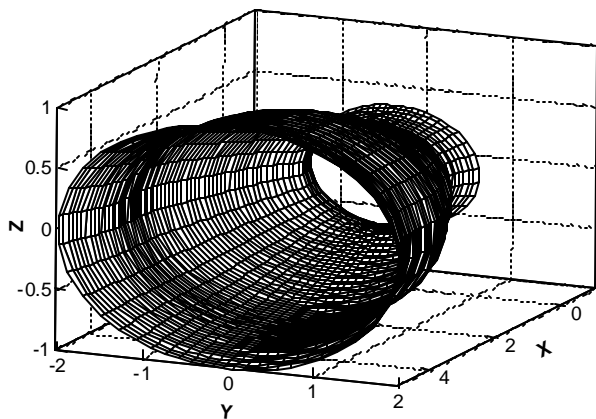


Fig 4.(b) Final shape of the 3D elliptical nozzle obtained by the hybrid method with inviscid flow

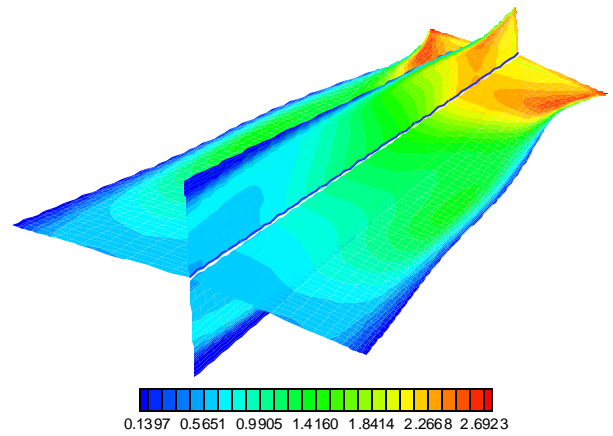


Fig. 5(a) Initial distribution of $\frac{ru^2 + p}{r_0 u_0^2}$ from inlet to outlet obtained with inviscid flow

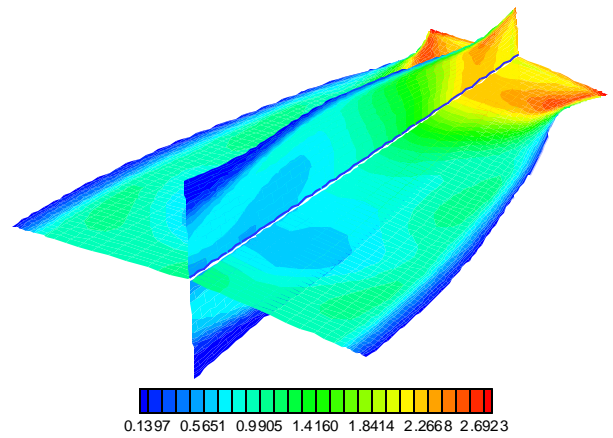


Fig. 5(b) Optimized distribution of $\frac{ru^2 + p}{r_0 u_0^2}$ from inlet to outlet obtained by the hybrid method with inviscid flow

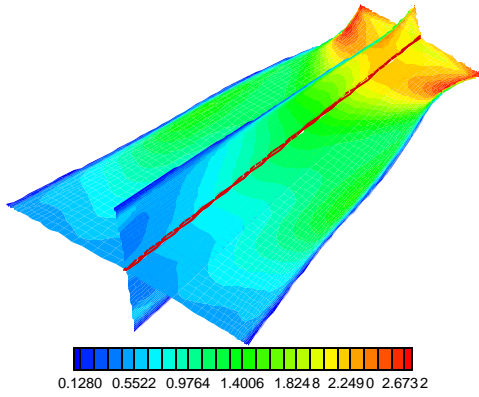


Fig.6(a) Initial distribution of $\frac{\mathbf{r}u^2 + p}{\mathbf{r}_0 u_0^2}$ from inlet to outlet
obtained with viscous flow

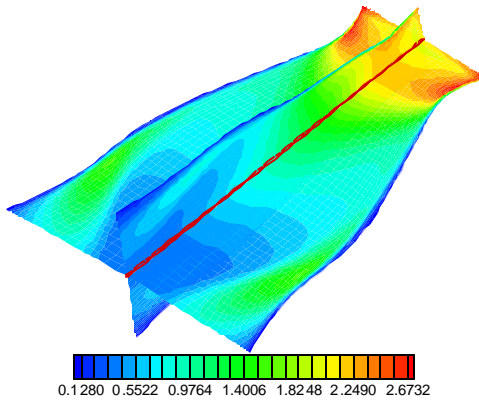


Fig.6(b) Optimized distribution of $\frac{\mathbf{r}u^2 + p}{\mathbf{r}_0 u_0^2}$ from inlet to outlet
obtained by the hybrid method with viscous flow

VI. CONCLUSION

The proposed hybrid optimization method combining the simultaneous perturbation stochastic approximation (SPSA) and gradient-based BFGS method has been investigated in the optimal design of a three-dimensional elliptical nozzle shape to improve thrust production. Its performance has been compared with those of simultaneous perturbation stochastic approximation, simulated annealing and gradient-based BFGS method. Comparison of these optimization methods using CFD solvers based on inviscid flow and viscous flow problems to evaluate the objective function has also been considered in this study. The numerical results show that the gradient-based method is the most efficient method for both inviscid and viscous flow solvers used in the design optimization. However using the gradient-based method may result in getting trapped into local minimum and this can be observed from the design results, shown in Table.1 and Table. 2. From the design results, it can be seen that the hybrid method has a high computational efficiency and that it can decrease computational cost significantly compared with stochastic

methods such as SPSA method and SA for the three-dimensional nozzle design for both inviscid and viscous flow solvers, and has almost same computational efficiency as the gradient-based BFGS method. Also the value of the optimised objective function computed by the hybrid optimization method is higher than those obtained by the other methods and may be closer to the global optimum. The hybrid method of BFGS-SPSA does take advantage of the high efficiency of the gradient-based methods, and the global search capability of SPSA method at the same time.

REFERENCES

- [1] Wang, X. and Damodaran, M., "Comparison of Deterministic and Stochastic Optimization Algorithms for Generic Wing Design Problems", *AIAA Journal of Aircraft* Vol. 37, No.5, 2000, pp.929-932.
- [2] Xing, X.Q. and Damodaran, M., "Application of the Simultaneous Perturbation Stochastic Approximation Method for Aerodynamic Shape Design Optimization", AIAA paper 2002-5643, 9th AIAA/ISSMO Symposium on Multidisciplinary Analysis and Optimization, 4-6 September 2002 / Atlanta, GA.
- [3] Xing, X.Q. and Damodaran, M., "Aerodynamic Shape Design Optimization Using Hybrid Stochastic and Deterministic Optimization methods and CFD", AIAA paper 2003-3786, 21th AIAA Applied Aerodynamics Conference, 23 -26 June 2003 / Orlando, FL.
- [4] Spall, J. C., "Multivariate Stochastic Approximation Using a Simultaneous Perturbation Gradient Approximation", *IEEE Transaction on Automatic Control*, Vol.37, No. 3, 1992.
- [5] Spall, J. C., "An Overview of the Simultaneous Perturbation Method for Efficient Optimization", *Johns Hopkins APL Technical Digest*, Vol.19, No.4, 1998, pp.482-492.
- [6] Spall, J. C., "Implementation of the Simultaneous Perturbation Algorithm for Stochastic Optimization", *IEEE Transactions on Aerospace and Electronic Systems*, Vol. 34, No.3, July 1998, pp.817-823.
- [7] Vicini, A., and Quagliarella, D., "Airfoil and Wing Design through Hybrid optimization strategies", *AIAA Journal*, Vol. 37, No. 5, 1999, pp. 634-641.
- [8] Poloni, C., "Hybrid GA for Multiobjective Aerodynamic Shape Optimization" in Winter G. et al, editors, *Genetic Algorithms in Engineering and Computer Science*, John Wiley & Sons Ltd., England, Dec, 1995, pp. 397-416.
- [9] Muyl, F., Dumas, L., and Herbert, V., "Hybrid Method for Aerodynamic Shape Optimization in Automotive Industry", presented in 3rd international conference of Applied Mathematics for Industry Flow Problems, 2002, Lisbon, Portugal.
- [10] Wang, X. and Damodaran, M., "Design Optimization of 3D Nozzle Shapes Using CFD and Parallel Simulated Annealing", AIAA paper 2001-0264, 39th AIAA Aerospace Sciences Meeting & Exhibit, 8-11 January, 2001, Reno, NV.
- [11] Press, W.H., Teukolsky, S.A., Vetterling, W.T., and Flannery, B.P., *Numerical Recipes in Fortran: The Art of Scientific Computing*, Second Edition, Press Syndicate of University of Cambridge, 1997.
- [12] Yoon, S., and Kwak, D., "Implicit Navier-Stokes Solver for Three-Dimensional Compressible Flows", *AIAA Journal*, Vol. 30, No. 11, pp 2653-2659, 1992.
- [13] Yee, H.C., and Harten, A., "Implicit TVD Schemes for Hyperbolic Conservation Laws in Curvilinear Coordinates", *AIAA Journal*, Vol. 25, pp. 266-274, 1987.